Laser-cooled atoms as a focused ion-beam source

J. L. Hanssen, J. J. McClelland,* and E. A. Dakin
Electron Physics Group, Center for Nanoscale Science and Technology, National Institute of Standards and Technology, Gaithersburg, Maryland 20899-8412, USA

M. Jacka
Department of Physics, University of York, Heslington, York YO10 5DD, United Kingdom
(Received 26 June 2006; revised manuscript received 9 November 2006; published 21 December 2006)

The evolving field of nanofabrication demands that more precise fabrication and evaluation tools be developed. We describe a method for creating a high quality focused ion beam with enhanced capabilities using an ion source based on laser-cooled neutral atoms in a magneto-optical trap. This technique will improve resolution and brightness beyond the current state of the art, can be used with the full range of atomic species that can be laser cooled and trapped, and will allow unprecedented control over the ion emission, allowing, for example, the production of single ions "on demand." We give estimates for the emittance and present a realistic ray tracing analysis of a basic focusing system demonstrating the feasibility of focusing the beam to a spot size of less than 10 nm.

DOI: 10.1103/PhysRevA.74.063416 PACS number(s): 32.80.Pj, 41.75.Ak

I. INTRODUCTION

As the field of nanotechnology advances, the need for new tools to perform precise tasks on the nanometer scale will continue to grow. In particular, it will become crucial to extend the capabilities of high brightness ion beams. Increasing the brightness of such beams will allow finer resolution with higher current improving both the fabrication and the imaging of nanoscale devices. Extending the range of elements that can be used to create ion beams will broaden both the fabrication and imaging possibilities of focused ion beams through, for example, enabling the use of inert species such as rare gases. Finally, having precise control of the position and number of ions within the beam allows for deterministic doping which will be necessary for the fabrication of a variety of nano-devices such as spin based quantum computers [1], single-atom transistors [2], single photon emitters [3], and single atom probes [4].

We propose an ion source that can accomplish all of these goals simultaneously. The magneto-optical trap ion source (MOTIS) is based on the ionization of magneto-optically trapped laser-cooled atoms. Due to the low temperatures associated with laser cooling, the ion beam originating from the MOTIS has a narrow angular spread (of order 10 μrad) and hence has a low emittance. This, in combination with the large currents achievable due to the high loading rate of a magneto-optical trap, means the MOTIS is a high brightness source that is capable of high current, high-resolution beams.

In addition to improving upon existing technology, this source expands the capabilities of focused ion beams to perform tasks that are important to the burgeoning field of nanotechnology. As the number of different atoms that can be laser cooled is quite large, using a MOTIS opens the door for many more atomic species to create ion beams. It is also possible to have greater control of the source current using advanced laser cooling techniques. This will allow for precise doping of samples down to the level of single ions with nanometer resolution.

In this paper, we describe the photoionization process that converts the magneto-optically trapped neutral atoms into an ion source. We give estimates, based on the initial size of the ion cloud and the energy distribution, that show the resulting beam has a low emittance. We also present a realistic ray tracing analysis of a simple focusing system and demonstrate that it is possible to focus the beam to a spot size of less than 10 nm.

II. BACKGROUND

For roughly 30 years, high-resolution focused ion beams (FIBs) have proven useful for a variety of tasks such as microscopy, lithography, micromachining (ion milling and material deposition), and dopant implantation [5]. Over the years, a number of ion sources have been developed for FIB applications, including gas-phase [6], plasma [7], and liquid metal [8]. Of all the sources developed so far, the liquid-metal ion source (LMIS) has proven the most useful and is the most widely utilized today. The usefulness of the LMIS, while being due in part to its practicality of implementation, stems fundamentally from its very high brightness. This brightness allows the production of focused ion beams with spot sizes on the order of 10 nm while maintaining currents in the range of 1 to 10 pA. These characteristics give FIBs the necessary resolution and ion currents to perform a range of state-of-the-art nanotechnology tasks, making them an indispensable component of today's nanotechnology toolbox.

Despite their widespread use, existing ion sources do possess some limitations that impede progress toward broader applications and higher resolution. Because of the need to wet a tungsten tip with a liquid metal, the number of different ionic species that can be implemented in an LMIS is somewhat limited. Ga is by far the predominant element used, though other species, including Ag, Al, Be, and Cs,

*Electronic address: jabez.mcclelland@nist.gov

have been demonstrated [5]. These often require special conditions, such as a very hot tip or mass separation elements in the optics column, and tend to have less output current, so their applications are limited. The LMIS also suffers from an extremely large energy spread, more than several eV, which is generally considered attributable to space charge effects occurring in the very small emission area on the surface of the emitter [9]. This energy broadening leads to chromatic aberration in the focusing optics that form the focused ion beam, limiting the achievable resolution and forcing a tradeoff between beam current and resolution. Gas-phase sources address some of these problems in that they can operate with light elements and have a narrower energy spread, on the order of 1 eV, but the current is significantly less, they do not work with heavy elements, and they are more complicated to operate. Plasma sources also overcome some of the problems of the LMIS, but the brightness is orders of magnitude less than the other two sources. A further practical issue relevant to liquid metal and gas-phase sources is that the nanometer-scale effective source size, required for the existing sources to have high brightness, translates into a very acute sensitivity to source positional stability, which becomes an issue in the construction of a FIB system. For these reasons, it is desirable to investigate alternative sources of ions for FIB applications that combine all the desirable characteristics into one source: high brightness; implementation of various ionic species, both light and heavy; low energy spread; and brightness not solely due to a tiny effective source size.

In considering a source, the key attribute that must be examined is the source brightness, since a high brightness allows a small focal spot with high current. The brightness of a source is inversely proportional to its phase space area, which is given approximately by the product of the cross sectional area of the source and the angular spread of the ions emitted. A high brightness source can thus be obtained by either a small effective area or angular spread. The present ion sources attain their brightness primarily through making the effective source size extremely small. For example, the effective source diameter for a gallium LMIS is on the order of 50 nm [10]. With such a source size, the LMIS achieves a phase space area of order 10^{-15} cm^2 sr, despite the fact that it has a fairly large angular spread with a half angle of roughly 25° [11]. The other existing sources tend to have similar properties. The gas-phase ion source has an effective source size on the order of 1 nm and an angular spread of approximately 25° [12], while plasma sources have a larger effective source size of 3–5 μm and an angular spread of around 6° [7].

In this paper, we discuss the magneto-optical trap ion source (MOTIS), an ion source that attains very high brightness by concentrating on reducing the angular spread of the ions rather than the source size. The source is based on the ionization of magneto-optically trapped laser-cooled neutral atoms. In contrast with the source proposed by Freinkman *et al.* [13], which relies on ionization of a laser-cooled atomic beam, the MOTIS takes advantage of the magneto-optical trap's ability to produce clouds of neutral atoms as small as 10 μm in diameter with temperatures in the range of 100 μK. Such a cloud of atoms, when ionized and accelerated, can result in an extremely bright ion beam. This brightness comes from an extremely narrow angular spread which is a direct consequence of the very cold temperature of the atoms. For this system, the angular spread of the beam goes as the square root of the ratio of the temperature to the beam energy. Therefore, for a source at 100 μK ($\approx$10 neV), the spread can be as low as 10 μrad for a beam energy of 100 eV. Coupled with a source size on the order of tens of micrometers, this leads to a phase space area on the order of 10^{-16} cm^2 sr. This estimate is an order of magnitude smaller than what is possible with existing sources. Thus, in principle, it is possible to create focused ion beams from a MOTIS with a resolution that is much better than present sources.

In addition to having the potential for better than state-of-the-art resolution performance, the MOTIS can provide a broader choice of elements and a lower energy spread than present sources. To date, laser cooling has been demonstrated for the alkali metals Li, Na, K, Rb, Cs, and Fr, the alkaline-earth metals Mg, Ca, and Sr, the metastable noble gases He, Ne, Ar, Kr, and Xe, the metals Al, Ag, and Cr, and the rare earths Er and Yb. This range of elements opens possibilities for doping and deposition, where the choice of element is crucial, and it is also advantageous for microscopy and micromachining where having the choice of a light or heavy element is desirable. Because of the extremely low temperatures of MOTIS ions, the energy spread is dominated by the extraction potential gradient across the finite source size. With typical source sizes, widths of 100 meV or less are possible, greatly reducing the effects of chromatic aberration and making the design of focusing optics less demanding. Additionally, the low energy spread allows the beam to be focused to the nanometer scale at energies much lower than conventional ion sources. This opens possibilities for much better control over the implantation depth of ions and the size of the damage regions associated with ion milling.

Perhaps the most interesting qualities of the MOTIS are the capabilities that are not possible with any other source. A consequence of the fact that a MOTIS begins with trapped neutral atoms is the simultaneous production of electrons and ions from the same source volume [14]. Therefore, assuming an appropriate optical design, with a simple reversal of voltage polarity, the ion source can be changed into an electron source. We should note that the lighter mass of the electron makes it more sensitive to stray fields and space charge effects making an electron source based on magneto-optically trapped atom more demanding. However, as discussed in Ref. [14], a useful beam of electrons can still be produced. This adds a major degree of flexibility to the source, and opens possibilities for combined imaging and doping or machining with a single source.

The MOTIS can also exert degrees of control over the ion beam through advanced laser cooling techniques. For example, the implementation of atom-on-demand techniques [15] would allow the controllable production of only a single ion at a time with greater than 99% probability. The result would be a deterministic source of ions that can be deposited at will within the resolution of the focused beam. Such a capability, which is impossible with present ion sources, would prove useful in a variety of technological and scien-

tific applications, such as controlled doping of nanostructures, fabrication of single-photon sources, and quantum information processing [16].

III. SOURCE PERFORMANCE ESTIMATES

The starting place for determining the quality of a beam produced from a MOTIS is a description of the cold neutral atoms in a magneto-optical trap (MOT). A MOT [17] can be created with any atom that has a closed (or nearly closed) strong optical transition in which the upper level has one unit of angular momentum more than the lower level. The geometry consists of three orthogonal pairs of counterpropagating laser beams intersecting at the center of a quadrupole magnetic field. The wavelength of the laser light is tuned close to but just below the resonance of the atom in use, creating a velocity-dependent force which slows the atoms. The magnetic field contributes position dependence to this force, creating a trap center within the overlap of the laser beams. While the detailed behavior of a MOT is somewhat complex, and more detailed discussions can be found elsewhere [18,19], for present purposes it is sufficient to work with typical characteristics found in most common MOTs. Generally speaking, the atomic cloud has a nearly Gaussian distribution in three dimensions with a diameter that can range from 10 μm to a few millimeters, depending on the magnetic field gradient, the light intensity, and the number of atoms in the trap. The temperature of the atoms is generally governed by the Doppler temperature associated with the laser-cooling transition, given by $\hbar\Gamma/2k_B$, where Γ is the natural transition rate for the cooling transition and k_B is Boltzmann's constant. This temperature is typically of order 100 μK ($\approx$9 neV) for most MOTs. While the Doppler temperature is generally cold enough for generating a high quality beam of ions, we note that, if desired, significantly colder temperatures can be achieved by applying more sophisticated laser cooling techniques, such as polarization-gradient cooling [20]. The steady-state number of atoms in a MOT can vary greatly, depending on the load rate and the loss rate, with maximal values greater than 10^9 atoms. Maximum densities are of order 10^{11} atoms/cm^3, limited ultimately by a repulsive force due to rescattering of spontaneously emitted resonant light and light assisted collisions [18]. As will be shown, these conditions can lead to ion currents in the nanoampere range.

In order to utilize the neutral atoms as an ion source, they must be converted into ions. The most efficient means of doing this is through photoionization, in which a high energy photon ejects an electron from an atom, leaving behind an ion [21]. This is accomplished by directing a laser beam at the atom cloud with photon energy equal to or greater than the difference between the excited state of the atom and the continuum. It is important that the photon have only the minimum energy necessary to accomplish this task for several reasons. First, this provides a means of selectively ionizing the atoms within the MOT. The photons only have enough energy to ionize excited-state atoms, ensuring that background atoms that are not in the MOT are not part of the ion beam. Secondly, any excess energy from the photon gets converted into kinetic energy of the ion-electron system. While the ion, being orders of magnitude heavier than the electron, receives little of the excess energy, it nevertheless can receive an amount that is substantial relative to the extremely cold temperatures involved. This excess energy results in a momentum kick to the ion in a more or less random direction. The result for a collection of ions is an increase in the width of the velocity distribution in both the longitudinal and transverse directions and hence an increase in the energy width. As an example of how large this effect can be, a gas of cold chromium atoms at 100 μK that is ionized by photons tuned 100 GHz (400 μeV) above the ionization threshold will have its energy width increased by a factor of 2, which is enough to reduce the quality of the ion beam. It should also be noted that it is not necessary to use only a single photon ionization process. Multiple photons with an energy sum equal to the ionization threshold can be used for the same purpose. This can be done nonresonantly or resonantly, where an intermediate excited state of the atom is used.

There are two useful quantities that characterize the quality of an ion beam, the normalized emittance ε and the brightness B. The unnormalized emittance is a measure of the phase space occupied by the beam, and is defined as [22]

$$\varepsilon_x' = \frac{1}{\pi}\left(\int\int dx dx'\right), \tag{1}$$

where x and x' are the transverse position and angular coordinates of the beam and the integration is over the position and angular distributions. This value will change with the beam energy; therefore, it is more useful to use the normalized emittance which is simply the emittance scaled by the square root of the beam energy U

$$\varepsilon_x = \varepsilon_x'\sqrt{U}. \tag{2}$$

It can be shown that the normalized emittance is an invariant quantity along a focusing column (neglecting aberrations and space charge effects) which allows for comparisons between different systems. Also, by knowing this value, it is possible to determine the final resolution of a system [11]. For a source in a field-free region with a Gaussian spatial distribution characterized by a standard deviation, σ_x ($1/\sqrt{e}$ radius), and a Maxwellian velocity distribution in the x direction characterized by a temperature T, Eqs. (1) and (2) reduce in the small angle limit to

$$\varepsilon_x = \sigma_x\sqrt{\frac{k_B T}{2}}. \tag{3}$$

Applying this expression to a chromium MOT with $\sigma_x = 5$ μm and $T = 100$ μK, Eq. (3) yields a value of $\varepsilon_x \approx 3.3 \times 10^{-7}\pi$ mm mrad$\sqrt{\text{MeV}}$. This normalized emittance is three times smaller than the measured normalized emittance value of $\varepsilon_x \approx 10.7 \times 10^{-7}\pi$ mm mrad$\sqrt{\text{MeV}}$ for a gallium LMIS operated in high resolution mode [23]. It is important to note that for the LMIS to reach its lowest emittance, the beam must be apertured, a process that reduces the current output to the order of 10 pA. For the MOTIS, the emittance is not reduced through aperturing, and therefore the emittance (and hence resolution) is independent of the current, provided space charge effects are negligible.

Using the emittance, we can calculate the expected attainable spot size with a MOTIS, assuming it is coupled with a typical focusing column. For a perfect lens, the spot size is entirely dictated by the emittance of the ion beam, but for a realistic lens, aberrations limit the final resolution. Spherical aberration and chromatic aberration are the leading effects that limit the resolution of FIBs. The final spot radius r_{total} is taken to be a root-power-sum of the various contributions including the radius due to spherical aberrationdss r_{SA}, the radius due to chromatic aberration r_{CA}, and the emittance limited radius $r_{\text{emittance}}$ [24]. Spherical aberration effects depend on the emission half-angle of the source, α, and contribute to the spot size according to

$$r_{\text{SA}} = \frac{1}{2} C_{\text{SA}} \alpha^3, \tag{4}$$

where C_{SA} is the spherical aberration coefficient [11]. While chromatic aberration is a major component of the spot size in conventional FIBs, it is completely negligible in the MOTIS because of the very low energy spread. Neglecting the chromatic aberration contribution, it can be shown that the minimum spot size for a given normalized emittance is

$$r_{\text{total}} = \gamma C_{\text{SA}}^{1/4} \varepsilon^{3/4} U^{-3/8}, \tag{5}$$

where γ is a numerical factor of order unity [25]. Using Eq. (5) with the above calculated emittance, a beam energy of 1 keV, and assuming a realistic spherical aberration coefficient of 200 mm rad^{-3} [26], we calculate a spot radius of approximately 3.8 nm.

While emittance highlights the quality of the beam, brightness measures the useful current that can be focused into a spot. It depends on the amount of current I that is emitted from an area A into a solid angle Ω and takes the form [9]

$$B = \frac{d^2 I}{d\Omega dA}. \tag{6}$$

Since the solid angle can change as a function of beam energy, a more useful quantity is the normalized brightness $\beta = B/U$. The normalized brightness is related to emittance by [22]

$$\beta = \frac{I}{\varepsilon_x \varepsilon_y}, \tag{7}$$

where ε_x and ε_y are the emittances in the two orthogonal directions transverse to the direction of propagation. This quantity is also invariant along the focusing column. Therefore, by knowing the brightness of a source it is possible to calculate how much current can be focused into a spot.

In order to calculate the brightness of a MOTIS, it is necessary to know the amount of current it can provide. The instantaneous current at a given time is given by the MOT population N_{MOT}, multiplied by the photoionization rate r_{ion} and the elementary charge e (assuming single ionization). N_{MOT} is determined by a rate equation that includes a loading term R_{load}, and loss terms associated with photoionization and the normal MOT lifetime τ_{MOT} due to other losses:

$$\dot{N}_{\text{MOT}}(t) = R_{\text{load}} - r_{\text{ion}} N_{\text{MOT}}(t) - N_{\text{MOT}}(t)/\tau_{\text{MOT}}. \tag{8}$$

Under steady-state conditions, the solution to this equation is $N_{\text{MOT}} = R_{\text{load}} \tau'$, where $\tau' \equiv \tau_{\text{MOT}}/(1 + r_{\text{ion}} \tau_{\text{MOT}})$. The resulting steady-state current is

$$I_{\text{SS}} = e r_{\text{ion}} R_{\text{load}} \tau'. \tag{9}$$

It is interesting to note that for $r_{\text{ion}} \tau_{\text{MOT}} \gg 1$, the MOT lifetime and ionization rate become immaterial, and the steady-state current reduces to eR_{load}.

Thus, to calculate the current from a MOTIS, it is necessary to know R_{load}, τ_{MOT}, and r_{ion}. R_{load} can vary widely, depending on the atom flux from the source, and MOT parameters such as magnetic field gradient, and laser power and detuning. Generally, the highest values that have been seen are of the order 10^9 atoms per second. The MOT lifetime can also range widely, depending on the atomic species and vacuum environment. Values up to several seconds are not uncommon, but lifetimes as short as a few milliseconds are also seen, for example, with an atom such as Cr, where there are optical leaks [27]. The photoionization rate is given by

$$r_{\text{ion}} = \rho_e \frac{\sigma I_{\text{laser}} \lambda}{hc}, \tag{10}$$

where ρ_e is the excited state fraction, σ is the ionization cross section, I_{laser} is the ionization laser intensity, and λ is the wavelength of the ionization laser [28]. This rate also clearly depends on the specifics of a given situation, but a generic maximum value of 2.5×10^6 s^{-1} can be estimated, assuming $\rho_e = 0.25$, $\sigma = 10^{-18}$ cm^2, $\lambda = 500$ nm, and a laser with 1 W of power in a beam with $1/e^2$ radius of 5 μm.

To make a generic estimate of the maximum possible continuous current from a MOTIS, we set $R_{\text{load}} = 10^9$ atoms per second, $\tau_{\text{MOT}} = 1$ s, and $r_{\text{ion}} = 2.5 \times 10^6$ s^{-1}. These values result in a current of 160 pA. We note that this scenario is well into the $r_{\text{ion}} \tau_{\text{MOT}} \gg 1$ regime, and the current is determined solely by the load rate. It is also interesting to note that the steady-state MOT population is only 400 atoms in this scenario, and the density of such a MOT with a 5 μm standard deviation is 7×10^{10} atoms/cm^3 [27]. The normalized brightness in this case, as calculated from Eq. (7), is 1.5×10^{11} A cm^{-2} sr^{-1} MeV^{-1}.

The MOTIS can also be operated in a pulsed mode, which might be advantageous because the MOT magnetic field can be gated off during ion extraction, and also because higher currents can be obtained, albeit for short periods of time. In this mode, the MOT is allowed to reach a steady-state population $N_{\text{MOT}} = R_{\text{load}} \tau_{\text{MOT}}$ with the photoionization turned off. Then the magnetic field is turned off and the photoionization laser is turned on long enough to ionize a significant fraction of the atoms. The trap is then allowed to reload, which takes a time of order τ_{MOT}. The current in this scenario is given by

$$I(t) = e r_{\text{ion}} R_{\text{load}} \tau_{\text{MOT}} \exp(-t/\tau'), \tag{11}$$

where the ionization is turned on at $t = 0$. The quantity of interest to calculate in this case is the average current per pulse. For example, if the photoionization laser is turned on

with a pulse width equal to τ', the average current for the pulse is given by

$$I_{\text{pulse}} = 0.632 e r_{\text{ion}} R_{\text{load}} \tau_{\text{MOT}}. \quad (12)$$

Inserting the above generic maximum values into Eq. (12) results in an average pulse current of 0.25 mA. While this current is quite high, the average pulse brightness is in fact limited in this case, because the MOT density is limited to a maximum of 10^{11} cm^{-3}. This density limit governs the minimum size of the MOT, given the number of atoms $N_{\text{MOT}} = R_{\text{load}} \tau_{\text{MOT}}$ that accumulate in the MOT when the ionization pulse is off. For the present example, we have $N_{\text{MOT}} = 10^9$ atoms, which, when combined with the density limit, requires the MOT to have a standard deviation no smaller than 610 μm. Despite this larger MOT size, the average pulse brightness is still quite high at 1.6×10^{13} A cm^{-2} sr^{-1} MeV^{-1}, a value that is two orders of magnitude higher than the steady-state value.

In addition to estimating generic maximum values, it is also of interest to make estimates for a different scenario, one that is closer to planned experiments in our laboratory. For this example we consider Cr atoms with $R_{\text{load}} = 10^8$ atoms per second, $\tau_{\text{MOT}} = 0.01$ s, and $r_{\text{ion}} = 2.5 \times 10^4$ s^{-1} [29]. These parameters still correspond to the $r_{\text{ion}} \tau_{\text{MOT}} \gg 1$ regime, so the steady-state current is $eR_{\text{load}} = 16$ pA. The number of atoms in the MOT is now 4×10^4, which dictates a standard deviation of 10 μm, based on a maximum density of 10^{11} cm^{-3}. The resulting steady-state brightness is 3.7×10^9A cm^{-2} sr^{-1} MeV^{-1}. Calculating for the pulsed mode, we assume as above a pulse width equal to τ' (40 μs in this case), and obtain a pulse-averaged current of 2.5 nA. N_{MOT} in this case is 10^6, resulting in a MOT standard deviation of 60 μm, because of the constraint on MOT density. The pulse-averaged brightness is then 1.6×10^{10} A cm^{-2} sr^{-1} MeV^{-1}.

The calculated values for these scenarios show that the MOTIS is indeed a high brightness source when operated in either a continuous or pulsed mode. Currents can be obtained that are more than an order of magnitude greater than the typical current of 10 pA obtained from an LMIS in high resolution mode, and predicted brightness values are significantly larger than the measured brightness values of a gallium LMIS (5.8×10^7 A cm^{-2} sr^{-1} MeV^{-1} [30]), gas-phase ion sources (2.0×10^{10} A cm^{-2} sr^{-1} MeV^{-1} [31]), and plasma sources (10^5 A cm^{-2} sr^{-1} MeV^{-1} [7]).

In both steady-state and pulsed modes of operation, there is the possibility of forming an unwanted background ion beam by two photon ionization of background gas atoms that are not part of the MOT. This multiphoton ionization can occur with either the MOT cooling and trapping light or the photoionization laser. In the case of multiphoton ionization of background atoms with the MOT light, the rate should be negligible. The intensity of the cooling and trapping light is over 6 orders of magnitude less than the photoionization laser resulting in a correspondingly lower ionization rate. In the case of multiphoton ionization of background atoms with the photoionization laser, the rate for this process to happen is strongly dependent on whether or not there is resonant enhancement. In the case of no resonant enhancement, the two photon ionization rate is approximately the single photon ionization rate squared divided by the frequency of the photon used. This is a reduction of approximately 11 orders of magnitude. If an excited state of the atom is near the energy of the ionization photon, a resonant enhancement can increase the two photon ionization rate. In this case, the ionization rate is approximately the single photon ionization rate squared divided by the frequency difference between the ionization laser and the resonant energy level. For a frequency difference of 1 GHz, this corresponds to a reduction of approximately 5 orders of magnitude. It should be possible to set the frequency of the laser such that the rate is exceedingly small and can be neglected. In either case, two photon ionization should be an insignificant effect.

It is also worth discussing the effect of the magnetic field necessary for formation of the MOT. While this field can be turned off during ion extraction in the pulsed mode, its effects must be considered if the source is to be operated in a continuous mode. A typical quadrupolar magnetic field used to create a MOT has a gradient of ≈ 0.2 T/m. The ion beam optical axis can be aligned with the field such that the velocity of the ions is parallel to the magnetic field, and hence, minimize the force on the ions. Since the beam does have a finite width, the ions will experience a small magnetic field perpendicular to their velocity. Based on a typical magnetic field gradient and a beam diameter of 50 μm the ions will see a peak magnetic field value of about ± 5 μT at the edges of the beam. The primary effect of this field is a small deflection, as well as a "twisting" of the beam around the axis of propagation. The size of the deflection depends on the beam energy and specific geometry of the ion optics. For the model system discussed in the next section, we estimate a deflection magnitude of about 2 μm. This deflection can be compensated by either electrostatic deflector plates or auxiliary magnetic field trim coils. Alternatively, the sample can be moved to match the position of the beam, so any deflection should not be a serious problem. There may, of course, be second order effects on the size of the focus that will need to be considered if the continuous mode is implemented.

In the discussion of emittance and brightness of the MOTIS so far, we have not taken into account the effects of space charge. For any ion source, mutual repulsion of ions within the beam causes some amount of beam expansion, resulting in a larger emittance, and also energy broadening. Whether these effects are negligible or not depends on the current density in the beam. In most situations the region of highest current density, usually located at the source, is the dominant source of space charge spreading and energy broadening [11]. A complete analysis of space charge effects is a complex task involving intensive calculations and is beyond the scope of this paper. We can, however, compare the MOTIS with other sources and carry out simple estimates to get some sense of how serious the effects are.

Based on the current estimates described above, we can calculate that the MOTIS has a maximum current density at the source no larger than 10^{-3} A/cm^2 in pulsed mode. This is nine orders of magnitude smaller than the LMIS, which has a typical current density of 10^6 A/cm^2 or higher, and is a result of the fact that the MOTIS obtains its small emittance from a small angular spread, not a small source area. This large disparity in current density suggests that space charge

effects will be much smaller than in the LMIS, whose space charge effects can be controlled sufficiently to yield 10 nm resolution.

To investigate this further, we carried out a simple numerical calculation in which the dynamics of a small group of ions with a spatial distribution corresponding to typical current densities achievable with the MOTIS were simulated in a field free space at an energy of 1000 eV. The results show that for a current of 10 pA, space charge effects increase the emittance by a factor of approximately three. As this calculation was done in a field free region, it should be considered as an overestimate, and the fact that the emittance did not increase much is indicative that space charge induced expansion will be at most a minor issue in the MOTIS.

To examine the space charge related energy spreading characteristics of the MOTIS, it is most useful to make a comparison with other sources based on current density. The LMIS, with a typical current density of 10^6 A/cm^2, has a minimum energy spread in excess of 5 eV, and gas-phase ion sources, with a typical current density of 1 A/cm^2, have an energy spread of about 1 eV. Since the MOTIS has a much lower current density of 10^{-3} A/cm^2, it is reasonable to expect that its energy distribution will not be affected much, if at all. To support this with a numerical rough estimate, it is possible to calculate an energy spread due to the combined effects of longitudinal relaxation and the "Boersch effect" (thermal relaxation between transverse and longitudinal degrees of freedom) [32]. Considering a generic 1000 eV, 10 pA beam of ions traveling a distance of 10 cm and starting with an initial source temperature of 100 μK, the estimated energy spread is 0.3 eV. (We note that this is an overestimate for the specific case described below since most of the time the ions are at a lower beam energy than 1000 eV, and these space charge effects are proportional to the square root of the beam energy.) This spread is of the same order of magnitude as the expected nominal 0.1 eV energy width of the MOTIS that arises from ionizing an atomic cloud of finite size within an extraction electric field. This suggests that space charge-induced energy spreading will not be a dramatic effect.

IV. RAY TRACING ANALYSIS

The emittance and brightness calculations described in the previous section suggest that a tight focus is possible with a MOTIS. To explore this further, we have performed realistic simulations of a model focused ion beam system using a ray tracing program based on finite difference electric field calculations and a fourth-order Runge-Kutta equation of motion calculation. A cylindrically symmetric electrostatic lens system, shown in Fig. 1, was modeled. The system is composed of three electrodes. The largest element is an 85 mm long tube with a 45° taper on one end. The taper is required to accommodate the laser beams necessary for forming the MOT. The tube has an inner diameter of 2 mm, an outer diameter of 10 mm, and is held at a voltage of −135 V. Surrounding the tube electrode is a sheath electrode held at ground potential to contain the fields of the electrostatic lens. Located behind the tube electrode is a planar electrode held

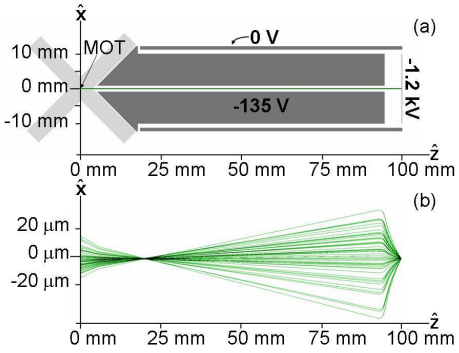

FIG. 1. (Color online) Lens geometry used in ray tracing simulations. (a) Scale drawing, showing electrostatic lens elements (dark gray) and MOT laser beams (light gray). The lens consists of three elements: a tapered cylinder held at −135 V, a grounded sheath surrounding the tapered cylinder, and a back plane held at −1.2 kV. At this scale, the atomic cloud is a small spot at the origin, and the ion trajectories lie along the horizontal axis (x=0 line). (b) Typical ion trajectories, with vertical axis expanded by a factor of 365. These trajectories, in green, were calculated for a MOT with a standard deviation of $\sigma_x=\sigma_y=\sigma_z=5$ μm and temperature of 100 μK. For clarity, only 50 of the 10 000 trajectories calculated are shown.

at a voltage of −1.2 kV. Magnetic fields were not included in the simulations.

In the simulation we calculated the trajectories for 10 000 ions. The ions were given a symmetric, three dimensional Gaussian spatial distribution of starting points defined by a standard deviation $\sigma=\sigma_x=\sigma_y=\sigma_z$, which was varied from 0.5 to 50 μm. To model the effects of source temperature, the ions were given a Maxwell-Boltzmann energy distribution with a fixed temperature that was varied from 10 μK to 1 mK. Self-interactions of the ions via Coulomb repulsion were not included in the simulation. Chromium ions were used in the simulation because of expertise with this element within our group [27]. The results are valid for any laser-cooled atom as the focusing properties of an electrostatic lens are not mass dependent [33].

Figure 1 shows the beam profile within the lens. The tapered front portion of the lens system extracts the ions and focuses them, forming a spot within a field free region approximately 14 mm behind the tip of the cone. This spot becomes an object that is subsequently imaged by a second lens formed in the gap between the exit of the first tube and the back electrode. The beam forms an image spot near the back electrode. Figure 2 shows an emittance plot of the beam at the focus near the back plane. For each ion, the angle of the trajectory with respect to the optical axis x' is plotted as a function of the transverse position x. From this plot it is possible to calculate the root-mean-square emittance via

$$\epsilon_{\text{r.m.s.}} = (\langle x^2\rangle\langle x'^2\rangle - \langle xx'\rangle^2)^{1/2}, \tag{13}$$

which has been shown to be equivalent to the emittance defined in Eq. (1) [25]. By taking the appropriate moments of the distribution, the plot yields a r.m.s. emittance of $\epsilon_{\text{r.m.s.}} = 1.2\times10^{-5}$ mm mrad, or 5.4×10^{-7} mm mrad $\sqrt{\text{MeV}}$ when

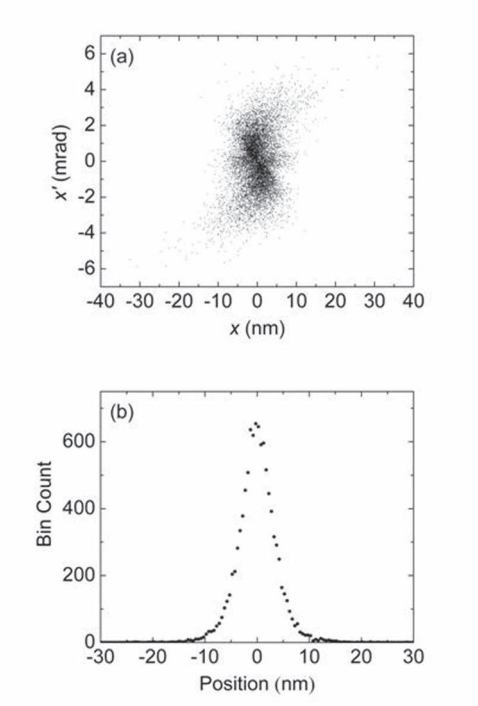

FIG. 2. Beam properties at the focus as calculated in the ray tracing analysis of our model system. (a) Emittance plot, showing trajectory angle (x') vs position (x) for 10 000 trajectories. (b) Transverse spatial distribution. Calculations were done with a source standard deviation of $\sigma_x=\sigma_y=\sigma_z=5$ μm and a source temperature of 100 μK.

normalized by the beam energy. This compares quite well with the value estimated above, especially considering that spherical aberrations from the focusing lenses are clearly playing a role, as evidenced by the S shape of the distribution in phase space [25].

Figure 2 also shows a plot of the spatial distribution at the focus, derived from a histogram of the ion positions. The full-width at half maximum (FWHM) of this distribution provides a measure of the spot size, which can then be investigated as a function of operating parameters of the source. Figure 3 shows a plot of spot size as a function of source temperature. The figure shows that the spot size monotonically increases as a function of atomic cloud temperature, as should be expected, since a higher temperature corresponds to a larger emittance. These data were generated with an initial source standard deviation of 5 μm. From Fig. 3, we see that a chromium MOT with temperature 100 μK and standard deviation $\sigma=5$ μm can produce a spot size of $\approx$7 nm. For temperatures lower than 10 μK, which can be achieved using more advanced laser-cooling techniques such as polarization gradient cooling [20], a resolution of 3 nm is possible. Furthermore, even if the MOT is operated suboptimally, and has a temperature as high as 1 mK, the system still has a resolution better than 20 nm.

The initial physical extent of the ion cloud is another parameter that determines the resolution of the beam. Figure 4 shows a plot of focal spot size as a function of initial cloud size. The focal size increases with increasing source diameter

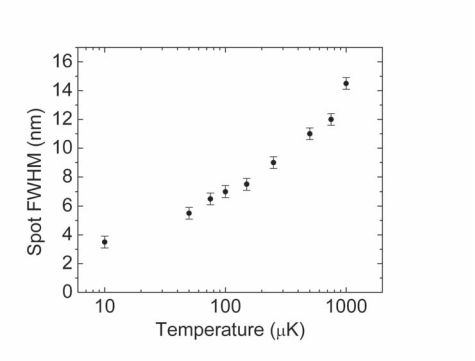

FIG. 3. Spot full width at half maximum (FWHM) as a function of source temperature, as calculated in the ray tracing analysis of our model system. The data were calculated with a source having a fixed standard deviation of $\sigma_x=\sigma_y=\sigma_z=5$ μm. Error bars indicate $\pm$ one standard deviation uncertainty in the calculated values (see text).

since emittance is linearly dependent on source size. On the low end, a focus of 4 nm is possible with an initial source σ of 0.5 μm. With a 50 μm source, the spot size is significantly larger at 50 nm, but still in the nanometer regime. The source size can be varied by either adjusting the diameter of the MOT, which is experimentally possible, or selectively ionizing a small portion of the atomic cloud by adjusting the waist of the ionization beam. Either way, the resolution can easily be adjusted through the ion cloud size.

The uncertainties indicated by error bars in Figs. 3 and 4 are intended to be interpreted as one standard deviation uncertainty, and arise from the binning used to create the histogram. The FWHM was measured as the distance between the midpoints of the two bins that are half the value of the maximum bin. A uniform distribution was assumed for the probability of the position of the half maximum point within the bin, giving rise to the uncertainty in the FWHM. For a tight focus, smaller bin sizes were used, allowing lower uncertainty in determining the width of the distribution. As spherical aberration and other effects spread the distribution out, larger bin sizes were used, leading to increased uncertainty in the measurement of large foci.

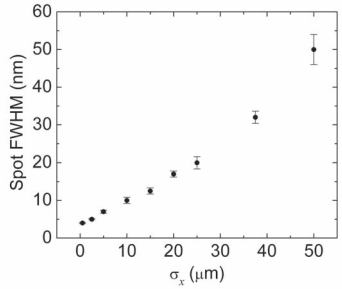

FIG. 4. Spot full width at half maximum (FWHM) as a function of initial source standard deviation $\sigma_x=\sigma_y=\sigma_z$, as calculated in the ray tracing analysis of our model system. The data was calculated with an initial source temperature of 100 μK. Error bars indicate one standard deviation uncertainty in the calculated values (see text).

V. CONCLUSION

In summary, laser-cooled atoms can serve as a source for a high quality focused ion beam. Given the cold temperatures accessible through laser cooling and trapping, a beam with extraordinarily low angular divergence is possible. This creates a beam with an emittance considerably smaller than conventional sources. Depending on the manner in which the source is controlled, a variety of different currents can be produced, leading to a high brightness beam better than the state of the art.

In addition to having the potential to produce a focused ion beam with better resolution and brightness than existing FIB sources, the MOTIS offers several advantages. The source has a much narrower energy width than other ion sources, resulting in much smaller chromatic aberration and a capability of nanoscale focusing at much lower energies. Because of the range of atoms amenable to laser cooling, an ion beam can be created from a larger selection of elements than is available with liquid metal, gas-phase, or plasma sources. These attributes could extend the usefulness of FIBs in areas such as microscopy and micromachining. Also, novel laser cooling techniques will allow for exotic ion beams to be created. Through atom-on-demand technology, a single ion can be placed with 10 nm resolution deterministically. This opens the door for new technological advances as well as new physics.

ACKNOWLEDGMENTS

We would like to thank Jon Orloff for fruitful discussions, and the members of the NIST Electron Physics Group for useful ideas and criticism.

[1] B. E. Kane, Nature (London) **393**, 133 (1998).
[2] J. Park, A. Pasupathy, J. Goldsmith, C. Chang, Y. Yaish, J. Petta, J. Sethna, H. Abruña, P. L. McEuen, and D. C. Ralph, Nature (London) **417**, 722 (2002).
[3] C. Kurtsiefer, S. Mayer, P. Zarda, and H. Weinfurter, Phys. Rev. Lett. **85**, 290 (2000).
[4] J. Michaelis, C. Hettich, J. Mlynek, and V. Sandoghar, Nature (London) **405**, 325 (2000).
[5] J. Melngailis, J. Vac. Sci. Technol. B **5**, 469 (1987).
[6] J. Orloff and L. W. Swanson, J. Vac. Sci. Technol. **15**, 845 (1978).
[7] S. K. Guharay, E. Sokolovsky, and J. Orloff, J. Vac. Sci. Technol. B **17**, 2779 (1999).
[8] L. R. Harriott, Nucl. Instrum. Methods Phys. Res. B **55**, 802 (1991).
[9] J. Orloff, Rev. Sci. Instrum. **64**, 1105 (1993).
[10] J. W. Ward, J. Vac. Sci. Technol. B **3**, 207 (1985).
[11] J. Orloff, M. Utlaut, and L. Swanson, *High Resolution Focused Ion Beams* (Kluwer Academic, New York, 2003).
[12] S. Kalbitzer and A. Knoblauch, Rev. Sci. Instrum. **69**, 1026 (1998).
[13] B. Freinkman, A. Eletskii, and S. I. Zaitsev, Microelectron. Eng. **73-74**, 139 (2004).
[14] B. J. Claessens, S. B. van der Geer, G. Taban, E. J. D. Vredenbregt, and O. J. Luiten, Phys. Rev. Lett. **95**, 164801 (2005).
[15] S. B. Hill and J. J. McClelland, Appl. Phys. Lett. **82**, 3028 (2003).
[16] T. Shinada, S. Okamoto, T. Kobayashi, and I. Ohdomari, Nature (London) **437**, 1128 (2005).
[17] E. L. Raab, M. Prentiss, A. Cable, S. Chu, and D. E. Pritchard, Phys. Rev. Lett. **59**, 2631 (1987).
[18] H. J. Metcalf and P. v. d. Straten, *Laser Cooling and Trapping* (Springer-Verlag, New York, 1999), and references within.
[19] A. M. Steane, M. Chowdhury, and C. J. Foot, J. Opt. Soc. Am. B **9**, 2142 (1992).
[20] J. Dalibard and C. Cohen-Tannoudji, J. Opt. Soc. Am. B **6**, 2023 (1989).
[21] G. Mainfray and C. Maus, *Multiphoton Ionization of Atoms* (Academic Press, Orlando, FL, 1984).
[22] R. Keller, *The Physics and Technology of Ion Sources* (John Wiley and Sons, New York, 1989).
[23] G. D. Alton and P. M. Read, J. Appl. Phys. **66**, 1018 (1989).
[24] J. E. Barth and P. Kruit, Optik (Stuttgart) **101**, 101 (1996).
[25] J. D. Lawson, *The Physics of Charged-Particle Beams* (Oxford University Press, New York, 1988).
[26] This is the numerically calculated value of the spherical aberation coefficient for the lens used in the simulations described in the paper.
[27] C. C. Bradley, J. J. McClelland, W. R. Anderson, and R. J. Celotta, Phys. Rev. A **61**, 053407 (2000).
[28] O. Marago, D. Ciampini, F. Fuso, E. Arimondo, C. Gabbanini, and S. T. Manson, Phys. Rev. A **57**, R4110 (1998).
[29] The ionization rate is based on chromium atoms being ionized by a 200 mW photoionization beam at a wavelength of $\approx$322 nm focused to a waist of 10 μm. A photoionization cross section of 10^{-18} cm^2, and an excited state fraction of 25% are assumed.
[30] R. L. Seliger, J. W. Ward, V. Wang, and R. L. Kubena, Appl. Phys. Lett. **34**, 310 (1979).
[31] J. Orloff and L. W. Swanson, J. Vac. Sci. Technol. **12**, 1209 (1975).
[32] Y. Zou, Y. Cui, V. Yun, A. Valfells, R. A. Kishek, S. Bernal, I. Haber, M. Reiser, P. G. O'Shea, and J. G. Wang, Phys. Rev. ST Accel. Beams **5**, 072801 (2002).
[33] E. Harting and F. H. Read, *Electrostatic Lenses* (Elsevier Scientific, New York, 1976).